Global parameter optimization for cardiac potassium channel gating models

Jeffery R. Balser, Dan M. Roden, and Paul B. Bennett

Departments of Medicine and Pharmacology, Vanderbilt University School of Medicine, Nashville, TN 37232

ABSTRACT Quantitative ion channel model evaluation requires the estimation of voltage dependent rate constants. We have tested whether a unique set of rate constants can be reliably extracted from nonstationary macroscopic voltage clamp potassium current data. For many models, the rate constants derived *independently* at different membrane potentials are not unique. Therefore, our approach has been to use the exponential voltage dependence predicted from reaction rate theory (Stevens, C. F. 1978. *Biophys. J.* 22:295–306; Eyring, H., S. H. Lin, and S. M. Lin. 1980. Basic Chemical Kinetics. Wiley and Sons, New York) to couple the rate constants derived at different membrane potentials. This constrained the solution set of rate constants to only those that also obeyed this additional set of equations, which was sufficient to obtain a unique solution. We have tested this approach with data obtained from macroscopic delayed rectifier potassium channel currents in voltage-clamped guinea pig ventricular myocyte membranes. This potassium channel has relatively simple kinetics without an inactivation process and provided a convenient system to determine a globally optimized set of voltage-dependent rate constants for a Markov kinetic model. The ability of the fitting algorithm to extract rate constants from the macroscopic current data was tested using "data" synthesized from known rate constants. The simulated data sets were analyzed with the global fitting procedure and the fitted rate constants were compared with the rate constants used to generate the data. Monte Carlo methods were used to examine the accuracy of the estimated kinetic parameters. This global fitting approach provided a useful and convenient method for reliably extracting Markov rate constants from macroscopic voltage clamp data over a broad range of membrane potentials. The limitations of the method and the dependence on initial guesses are described.

INTRODUCTION

Ion channel gating models are useful for quantitatively describing gating behavior and drug-channel interactions, providing clues to channel structure, and serving as aids in the design of experimental tests to further probe their behavior (Hodgkin and Huxley, 1952; Armstrong, 1981; Hille, 1977; Hondeghem and Katzung, 1977; Stuhmer et al., 1989). Most voltage-gated ion channels in excitable cells can be described in terms of Markov models where the open and closed states are interconnected by rate constants which are functions of membrane potential but are not functions of time (Ross, 1972; Colquhoun and Hawkes, 1983; Korn and Horn, 1988; McManus et al., 1988; for exception, see Liebovitch and Sullivan, 1987). The voltage dependence of the rate constants arises from sensitivity of the channel protein conformational changes to the transmembrane electrical field. Thus, either formal charges or dipoles within the protein structure are influenced by changes in the membrane potential and the rate constants characterize the energy barriers separating the channel conformers.

Horn and colleagues (1984, 1987) have recently made significant progress in the development and selection of kinetic models using single-channel data. While single-channel observations can, in some cases, provide a direct measure for specific rate constants in a kinetic model, it is often impossible to obtain sufficient data to fully determine all the kinetic parameters for a gating model over a wide voltage range (Horn and Vandenberg, 1984; Kunze et al., 1985). Bauer et al. (1987) recently pointed out that stationary single channel data are "not a particularly rich source of information about the kinetics of channel gating" when trying to determine rate constants for complex gating models; and that nonstationary data provide an additional source of kinetic information. They suggest that for ion channels with only one open state there is sufficient kinetic information in the observed open channel probability time course to extract rate constants from a Markov model provided certain conditions can be fulfilled. Appropriately scaled macroscopic current represents the average nonstationary probability of channel opening as a function of time at a particular membrane potential, and thousands of single channel records may be required to obtain the the same kinetic information.

Address correspondence to Dr. Paul B. Bennett, CC-2209 Medical Center North, Vanderbilt University, Nashville, TN 37232.

Furthermore, some ion channels, such as delayed rectifier potassium channels in heart, are present in low numbers in the cell membrane (Clapham and DeFelice, 1985), and are therefore very difficult to characterize using single channel recording methods. Thus, an approach for extracting useful kinetic information from macroscopic data is needed.

Two central questions are addressed in this paper: Can a unique set of rate constants be reliably extracted from nonstationary macroscopic voltage clamp current data? To what degree of certainty can the rate constants be estimated? It should be pointed out that we have not attempted to select among various models. This structural identifiability problem is addressed very elegantly by Horn and colleagues (1984, 1987) for certain ion channel models.

To address these questions we have developed a *global* fitting procedure to extract the rate constants of a given Markov model from macroscopic ion channel currents in voltage-clamped membranes. The term global implies using comprehensive data sets which include experimental information from a broad range of conditions (membrane potentials, etc) to limit the possible solutions for the model system. This assumes that there is information contained in the data that can constrain a fit and that this information is lost if a model is fitted at each membrane potential individually. Thus, the fitting algorithm selected rate constants from the solution set of all possible rate constants that can describe the data by constraining the possible solutions to be exponential functions of membrane potential as predicted from reaction rate theory (Eyring et al., 1980; Stevens, 1978). This approach reduced the number of possible solutions and allowed convergence to a unique set of rate constants that fulfill the constraints of the data and the predefined voltage dependence. To test this global fitting approach for kinetic analysis of macroscopic currents, we have analyzed whole-cell delayed rectifier currents measured in voltage-clamped guinea pig ventricular myocytes with the three-state Markov model described by Bennett et al. (1985, 1986). This simple model was used because the analytical solution is known. However, because the analytical solutions are not possible for most other more complicated channel models, we used numerical integration methods for the sake of generality in extending this approach to more complex models. Using this model, we first fit K currents from guinea pig ventricular myocytes to obtain reasonable parameters for further simulations. The fitted parameters were then used to synthesize ensembles of macroscopic currents. These simulated data sets were then subjected to the global fitting procedure to test whether the known rate constants could be extracted reliably. Monte Carlo methods (Motulsky and Ransnas, 1987; Horn, 1987) were used to determine the accuracy

with which the rate constants could be extracted from whole cell currents by using the global fitting approach. The "robustness" of the method was tested using randomly selected initial guesses during multiple fitting runs to determine the ability to converge to a unique solution.

METHODS

Cell preparation and voltage clamp experiments

Guinea pig ventricular myocytes were obtained using a Langendorff perfusion technique similar to that described by Mitra and Morad (1985). Isolated cells were stored for subsequent use at 37°C as described elsewhere (Roden et al., 1988). To isolate potassium (K) currents and to eliminate non-K currents during depolarizing voltage steps, cells were superfused in a solution containing (in millimolar) N-methyl-d-glucamine 150, KCl 4.5, $MgCl_2$ 2.0, $CaCl_2$ 0.1, $CdCl_2$ 0.1, glucose 12.5. The pH of this solution was 7.4 and the temperature was 23°C. $LaCl_3$ (30 μM) was added to the external solutions to remove component(s) of a time-dependent current that contaminates the delayed rectifier current (Balser and Roden, 1988). Sodium currents were eliminated by the replacement of sodium by N-methyl-d-glucamine. Calcium-dependent currents were eliminated by the combination of a low external calcium concentration, the presence of the Ca channel blockers Cd^{++} and La^{+++}, and intracellular EGTA. Macroscopic currents were measured using the standard whole-cell configuration of the patch-clamp technique (Hamill et al., 1981). Patch electrodes measured 4–8 MΩ and contained (in millimoles per liter) KCl 150; $MgCl_2$ 2; N-2-hydroxy-ethyl-piperazine N'-2-ethanesulfonic acid (Hepes) 10; $CaCl_2$ 1; ethylene glycol-bis-(β-aminoethyl ether N,N,N',N'-tetraacetic acid (EGTA) 11; MgATP 5; K_2ATP 5. The pH was adjusted to 7.2 with potassium hydroxide. The largest K currents in these experiments were usually <300 pA and required >1 s to reach this magnitude. If the pipette access resistance tripled after GΩ seal formation and patch rupture, then without any series resistance compensation the voltage drop across the access resistance was <8 mV. The effects of this series resistance could be partially compensated using series resistance compensation circuitry in the Axopatch amplifier which reduced the actual voltage errors to <5 mV. Whole cell current records were filtered at 50–100 Hz (−3 dB; four-pole Bessel filter), digitized at 150–200 Hz and stored on the hard disk drive of an IBM PC/AT computer. The digitized records were subsequently digitally filtered at 10 Hz before analysis. This filtering did not compromise measurement of the channel gating kinetics; the smallest system time constant

(fastest component) corresponded to a frequency component of <5 Hz.

Models

Analytical solutions for the rate constants of all but the simplest state models cannot be derived without making simplifying assumptions. Hence, the evaluation of realistic models of channel gating requires numerical methods.

In the general case of a Markov gating model with N states, the probability of occupying a particular state, P_i, at any time, t, and voltage, V, is determined by a system of linear first-order differential equations. For such a gating model, where each state is potentially connected to all other states, the equations are as follows:

$$dP_i/dt = - \sum_{j=1}^{N} [k_{ji} \cdot P_i(t, V)]$$
$$+ \sum_{j=1}^{N} [k_{ij} \cdot P_j(t, V)] \quad i = 1, 2, \ldots N - 1; i \neq j \quad (1)$$

$$dP_N/dt = - \sum_{j=1}^{N-1} [dP_i/dt]. \quad (2)$$

k_{ij} is the rate constant leading to state i from state j, and is a function of membrane potential.

In a three-state catenary model for the delayed rectifier (Bennett, et al., 1985), the state diagram and the system of equations are as follows:

$$C_1 \underset{k_{12}}{\overset{k_{21}}{\rightleftharpoons}} C_2 \underset{k_{23}}{\overset{k_{32}}{\rightleftharpoons}} O_3$$

$$dP_1/dt = -k_{21}P_1 + k_{12}P_2 \quad (3)$$

$$dP_2/dt = k_{21}P_1 - (k_{12} + k_{32})P_2 + k_{23}P_3 \quad (4)$$

$$dP_3/dt = -dP_1/dt - dP_2/dt. \quad (5)$$

As shown, this system of three simultaneous differential equations has four unknown rate constants; hence at any single membrane potential the system is underdetermined with respect to the rate constants. Unique values of the rate constants which define the probability of occupying the open state at a single membrane potential cannot be determined. Therefore, a unique solution for the rate constants cannot be found when fitting the integrated solution for the open state $P_3(t, V)$ to the time course of the macroscopic current at a single membrane potential because multiple correct solution sets exist. The rate constants found by a parameter search procedure will thus depend on the initial parameter guesses. The problem of underdetermination at single membrane potentials increases as more states and rate constants are added.

To circumvent this problem, we developed a procedure that globally fits the time course of the macroscopic data at several membrane potentials simultaneously. We made

the standard assumption that the transmembrane electric field can promote or impede both formal and induced charges (or dipoles) in the protein and the rate constants for surmounting these energy barriers are described from reaction rate theory (Eyring et al., 1980) by a form of Eq. 6. Thus, the rate constants (k_{ij}) were expressed as functions of membrane potential as described by Stevens (1978):

$$k_{ij} = \exp \{A_{ij} + B_{ij} V + C_{ij} V^2\}. \quad (6)$$

This formulation indicates that the rate of transition between two states depends on the electrical field across the channel (V) and on three parameters (A_{ij}, B_{ij}, C_{ij}) that describe the potential energy barriers between the states. A_{ij} reflects the energy barrier height in the absence of an electrical field, B_{ij} represents the energy barrier height that exists due to charge-field and dipole-field interactions, and C_{ij} represents the contribution of total distortion polarization or field induced dipoles. In the limiting case of a low transmembrane field strength, the squared voltage term may not be required, and Eq. 6 may be simplified to the following form:

$$k_{ij} = \exp \{A_{ij} + B_{ij} V\}. \quad (7)$$

Either of these additional equations was sufficient to constrain the possible solutions for the rate constants.

In the three-state model discussed above with the four independent rate constants (k_{12}, k_{21}, k_{23}, and k_{32}), if the rate constants were expressed as two or three parameter functions of voltage, there were eight (A_{ij}, B_{ij}) or twelve (A_{ij}, B_{ij}, C_{ij}) free parameters for fitting. While this situation is grossly underdetermined at a single membrane potential, these parameterizations allow us to simultaneously fit the time course of the macroscopic currents at multiple membrane potentials. Because three equations describe the system at each membrane potential, by fitting "globally" at four or more membrane potentials we solve 12 or more equations in either 8 or 12 unknowns; hence, the system is fully determined. Although many of these concepts are well known, we are not aware of the previous utilization of the voltage dependence predicted from reaction rate theory to constrain the rate constants.

Global fitting procedure

To fit Markov state models to whole-cell data, it was first necessary to scale the macroscopic current into open state probability. Fig. 1 illustrates the estimation of steady-state activation by analysis of tail currents which eliminate the differences in driving force among activating voltages. Potassium current was activated by a 6-s voltage clamp step to membrane potentials between -20 and $+70$ mV and then membrane potential was stepped to
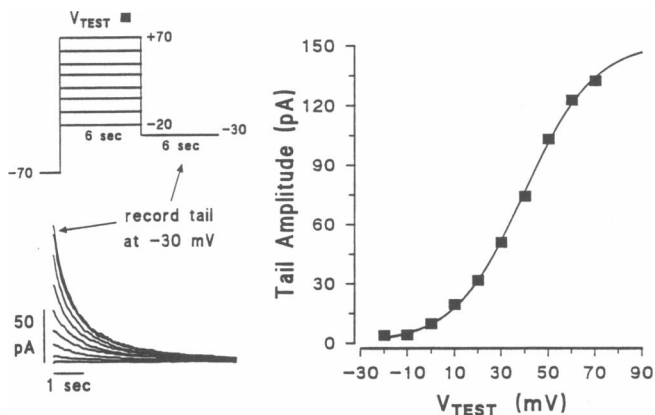
FIGURE 1 (*Left*) Deactivating K current tails recorded at −30 mV. Steady-state activation of K current was achieved at different membrane potentials (−20 to +70) before measuring the current tails at −30 mV. (*Right*) The tail amplitudes (*squares*), measured as the difference between the peak current at the beginning of deactivation and the steady-state current after 6 s at −30 mV, are shown as a function of activating voltage. The solid line indicates the nonlinear least-squares fit of a three-parameter Boltzmann equation to these data as described in the text.

−30 mV. The amplitudes of the deactivating tail currents at −30 mV were then measured (*left*) and were plotted as a function of the activation test voltage (V_{test}) to estimate the steady-state activation curve (*right*). Because the channels do not inactivate, the maximum steady-state probability of channel opening (at membrane potentials > +70 mV) was estimated by fitting the steady-state activation curve with the Boltzmann equation:

$$P_{open}(V) = I_{measured}/I_{max} = [1 + \exp((V_{1/2} - V)/sf)]^{-1}.$$

The fitted value of I_{max} was used to normalize the current data into probability of opening. The Boltzmann equation was used because it conveniently provided a good fit to the data and at steady state, the system can be partitioned into two pools, open and not open. Because we were only interested in an objective means to obtain I_{max} for normalization purposes, the Boltzmann equation was adequate.

The global fitting procedure involved repeatedly comparing the open state occupancy of the model with that of the data and revising the rate constant estimates iteratively. Numerical integration was utilized to calculate the open-state occupancy for each set of rate constants during each iteration. For selected cases, simple Runge-Kutta methods were adequate; however, in some cases at certain membrane potentials the differential equations become stiff; that is, the time scales on which the state occupancies change may differ by orders of magnitude at particular membrane potentials, thereby causing roundoff or

truncation errors to propagate through the solution (Press et al., 1986). Therefore, a numerical integrator, based on the original work on stiff differential equation solutions by Gear (1971), was utilized which automatically employs method switching for stiff and nonstiff problems (LSODA; Hindmarsh, 1983; Petzold, 1983). For the parameter searches described here, the Marquardt-Levenberg algorithm (Marquardt, 1963; Bevington, 1969) for minimizing the residual sum of squares was used due to its relative speed and convenience. These numerical procedures were incorporated into a general purpose FORTRAN program (GLOBAL) which fits gating models with up to six kinetic states. In addition to the delayed rectifier K channel model described here, we have used this procedure to evaluate kinetic parameters describing gating models for the cardiac Na channel (Bennett et al., 1989); for such models where the probability of occupying the fitted state (open state) increases and subsequently decreases at a single membrane potential, the Marquardt algorithm frequently diverged. Therefore, we have also implemented the GLOBAL software with a simplex parameter search algorithm (Nelder and Mead, 1965). The advantage of the simplex algorithm is that it rarely diverges (Caceci and Cacheris, 1984), however, it converges on a solution very slowly and global fits to a single data set required up to 1 wk on a VAX 8800 (Digital Equipment Corp., Malboro, MA). While this approach remains practical for fitting limited numbers of experimentally derived data sets, a Monte Carlo analysis requires fits to hundreds of simulated data sets. Therefore, for this statistical analysis of the global fitting approach we have used the Marquardt parameter search algorithm and a gating model that does not include macroscopic inactivation.

The global fitting procedure is computationally demanding due to the necessity of repeated numerical evaluation of a system of differential equations each time the kinetic parameters are updated by the search algorithm. Hence, globally fitting multiple sets of simulated macroscopic data at different membrane potentials, each containing up to 1,000 data samples, required unacceptably long execution times. We have therefore reduced the data sets for fitting purposes. In the Monte Carlo analysis described below, 32 sample points were selected to represent the macroscopic current at each membrane potential, and four activating and four deactivating membrane potentials ranging from −50 to +70 mV were chosen to represent a broad range of kinetic behavior. To appropriately represent kinetic features present in both of the time constants inherent in the three-state model, at each of the eight membrane potentials we calculated the two system time constants for the three-state model from the rate constants. We then collected 16 equally divided samples with a sampling interval equal to one-fourth of faster time

constant ($\tau_{fast}/4$) at each membrane potential to represent the early part of the ensemble current. The next 16 samples were equally spaced over a duration of four of the slower time constants ($\tau_{slow}/4$) at each membrane potential. From the Nyquist sampling theorem, the highest frequency signal detectable from a sampled data set is equal to or less than one-half of the sampling frequency; hence, the highest frequency we could detect after data reduction in this manner was $\{2 \cdot \tau_{fast}\}^{-1}$ which was twice the highest frequency component in the data.

Monte Carlo analysis: simulation of macroscopic data

A standard method for determining parameter uncertainty involves obtaining replicate observations of experimental data. Monte Carlo simulations can be used to investigate the statistical properties of model equations in a similar manner (Hammersley and Handscomb, 1964). The procedure involves using known parameters to generate large numbers of simulated data sets from the model equations and then subjecting these data sets to the standard form of analysis. In our case, we have assessed the ability of the global fitting procedure to extract the known rate constants from these simulated data sets.

Rather than arbitrarily choose rate constants to simulate a channel model for Monte Carlo analysis, we first globally fitted voltage-clamp data with a three-state model to obtain a reasonable set of parameters for generation of simulated data sets. Thus, the known rate constants that generated the simulated data sets provided a reasonable representation of potassium channel behavior. Single channel behavior was then simulated by randomly selecting the occupancy times for the various states at each membrane potential from the known distributions of lifetimes (DeFelice and Clay, 1983).

In this fashion, 90 data sets, each containing "whole cell" ensemble average currents were generated from the average of 1,000 single-channel simulations at eight different membrane potentials. Each of these 90 data sets was then separately subjected to the global fitting procedure; this allowed us to assess the variability in the rate constants when the true rate constants underlying the "channel" behavior were known. A similar analysis was performed on nine simulated data sets, each consisting of ensemble currents at the same eight voltages generated from 10,000 single channel simulations. Approximately 200 computer h were required for the entire analysis (enhanced IBM ATs running at 8.5–10 MHz with 80287 coprocessors).

During the fitting process, estimates of the standard errors of fitted parameters were calculated from the covariance matrix [the inverse of the curvature matrix, as described for the Marquardt fitting algorithm in Beving-

ton (1969)]. In general, for nonlinear models, the errors in the parameters are neither additive nor symmetrical and it is impossible to calculate exact confidence limits. The errors obtained from the covariance matrix are based on linearizing assumptions and underestimate the true uncertainty in the parameters (Motulsky and Ransnas, 1987; Bevington, 1969). Furthermore, we have fitted a set of parameters which defined the voltage dependence of the rate constants, not the rate constants directly (see Eq. 6). Because the models we have used, and because other more complicated nonlinear models have parameters that depend on each other in unknown ways, it is impossible to translate the errors in the fitted parameters into errors in the rate constants. We felt the most reliable way to obtain an estimate of the errors in the derived rate constants was to use Monte Carlo methods.

Sensitivity to initial guesses

It was also important to estimate to what extent the fitted parameters were sensitive to their initial guesses, or in other words, to test the robustness of the global fits. A standard error was calculated from the variance (the diagonal of the covariance matrix) obtained during fitting the three-state model to the experimental data set. These estimated parameter errors (EPE) provided a rough guide to the distribution of the estimated parameters. Therefore, we used these to explore the limits of the distribution to determine the extent to which initial guesses (parameters) might be varied from the known solution (global minimum). Initial guesses for each parameter were randomly selected 20 times from this distribution at a certain fraction (F) of the EPE. A synthesized data set using 1,000 channels as described above was then fitted with each of the 20 initial guesses. The fraction (F) of the parameter error was then incremented, and another set of 20 initial guesses was generated and used for fitting. The analysis was repeated until the initial guesses were sufficiently far from the correct solution that divergence of the fitting procedure or convergence to local minima consistently occurred.

Note that the convention for naming the rate constants (k_{ij}) differs from that given in Bennett et al. (1985, 1986). In this paper we have conformed to the standard matrix notation for subscripts. Thus, k_{ij} is the rate constant going to state i from state j. This convention preserves the proper position in the matrix formulation of the state equations, thus rate constant k_{12} is in the first row and second column of the rate constant matrix.

RESULTS

Rather than simply generate arbitrary rate constants for a Monte Carlo analysis, we first used the global fitting

procedure to fit whole-cell K current data to obtain a set of voltage dependent rate constants that reasonably described the channel kinetics (see Fig. 1). Fig. 2 shows examples of the currents elicited by activating clamp steps (*left*) from −70 to +10, +30, +50, and +70 mV and deactivating clamp steps (*right*) from +50 to +10, −10, −30, and −50 mV. The digitized data (*noisy traces*) are shown with the superimposed circles indicating the reduced data sets used in the global fitting procedure. The smooth solid lines indicate the global fit to these data using the three-state model, with a two-parameter expression describing the voltage-dependence of each of the four rate constants (Eq. 7). The dashed lines indicate the fit to the same data using the three parameter expression for the voltage dependence of the rate constants (Eq. 6).

Using the rate constants obtained in this manner, we then generated 90 simulated data sets, each containing the ensemble average open state probability from 1,000 simulated single channels. Fig. 3 (*top*) shows the records from two simulated data sets using the two parameter expression for the rate constants (Eq. 7) at the four activating and deactivating membrane potentials used previously for fitting the experimental data (Fig. 2). The stochastic nature of the channel gating is apparent as

FIGURE 3 (*Top*) Records from two superimposed simulated data sets at four activating and deactivating membrane potentials. Note the gating fluctuations that are obvious from the relatively small number of channels. (*Bottom*) Data samples taken from 1 of the 90 simulated data sets for fitting purposes (*circles*) are shown; the solid lines indicate the global fit to the simulated data. This analysis was repeated for each of the 90 simulated data sets. Apparent deviations of the lines from the data (*circles*) result because of the intrinsic channel gating fluctuations (*top panel*). The line will pass through the averaged data but not necessarily through the samples of a given single data set.
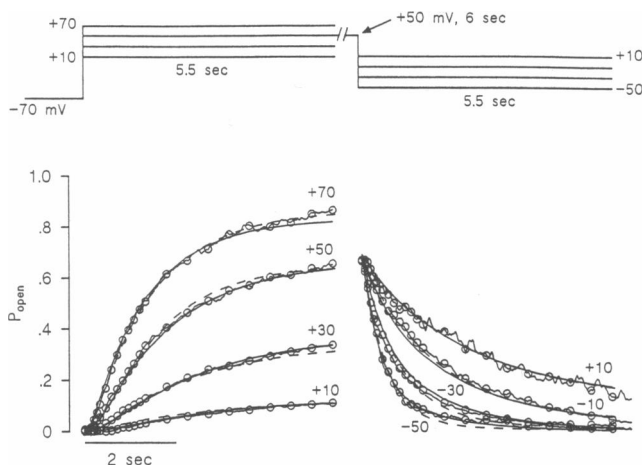

FIGURE 2 Time course of probability of channel opening obtained from macroscopic K current at different membrane potentials. The currents during voltage clamp steps from −70 to +10, +30, +50, and +70 mV (*left*) and deactivating clamp steps (*right*) from +50 to +10, −10, −30, and −50 mV were scaled into open channel probabilities by the best-fitting estimate of I_{MAX} obtained from the Boltzmann equation. The noisy tracings show the data, the open circles indicate data selected for the global fitting procedure. The smooth lines indicate a fit to the data using the two-parameter voltage dependence of the rate constants. The dashed lines indicate the fit to the same data using the three-parameter expression for the rate constants. The residual sum-of-squares for the fits using the two- and three-parameter expressions for the voltage dependence of the rate constants were 0.054 and 0.040, respectively.
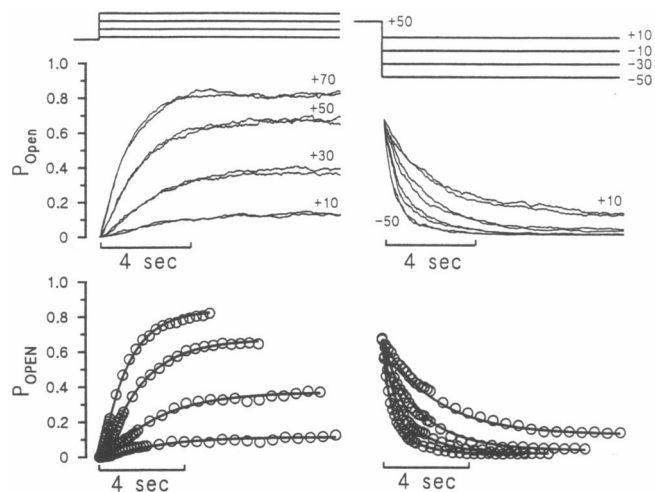
"noise" in these ensemble averages and it appeared similar to the channel fluctuations in the experimentally measured currents shown in Fig. 2. This suggests that 1,000 channels per cell reasonably approximates the experimental situation for the delayed rectifier K currents in these guinea pig myocytes. An analysis of channel number by nonstationary fluctuation methods (Sigworth, 1980) usually provided estimates ranging from 1,000 to 5,000 delayed rectifier channels per cell (unpublished observations). Two superimposed tracings are shown at each potential to emphasize the variability among different data sets; this variability leads to the uncertainty in the fitting process.

The bottom panels of Fig. 3 show the data samples taken from one of the ninety simulated data sets for fitting purposes; the lines indicate the global fit to these simulated macroscopic data. An identical analysis was carried out for all 90 data sets, thereby providing for statistical analysis 90 sets of fitted parameters describing the four system rate constants. The data synthesized from known rate constants allowed us to test the ability of the global fitting procedure to extract the same rate constants from these data.

An important aspect of fitting models to data is to determine whether the results depend on the initial guesses used to begin the fitting process. If they do then

the fitted results are not unique, and they represent parameters found in a local minimum of the sum-of-squares surface rather than the global minimum that is desired. We tested the dependency of the answers on the initial guesses as described in Methods. Table 1 shows the results obtained at the sum-of-squares global minimum and the percentage deviation away from these values that were used as initial guesses to test the ability of the fitting algorithm to find the global minimum. When initial guesses were >0.5 times the maxima shown in Table 1, convergence became increasingly rare. With these very poor guesses the fit would often diverge and cause the numerical integrator to become unstable. This is a severe test of the robustness of the fit because in many cases the guesses were quite far from the true value (up to 18,750% different, see Table 1). A typical approach for selecting initial guesses would be to take values that would as closely as possible approximate the data based on an "intelligent guess." The more systematic approach that we have adopted indicates that certain guesses are bound to fail at least with the Marquardt algorithm that we have used. In practice, 70% of the randomized initial guesses that were within a fraction of 0.25 of the maximum deviations listed in Table 1 converged to the global minimum. Thus, guesses in some cases as bad as 9,000% away from the global minimum, and more typically guesses >100% away from the global minimum would converge. The results indicate that care must be taken to ensure that a global minimum has been achieved, and the results obtained in practice will depend on the parameter search algorithm used.

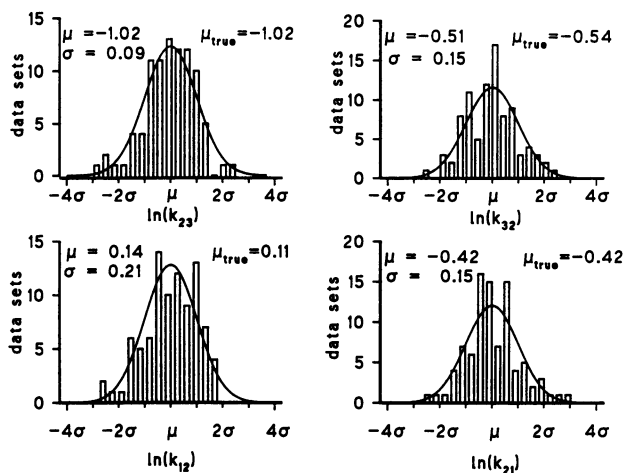The frequency distributions for each of the rate constants from the model with two parameters per rate

FIGURE 4 Relative frequency distributions for each of the four rate constants at +30 mV derived from fitting 90 data sets are shown. The values of μ and σ (means and standard deviations) obtained from fitting each distribution with a Gaussian function are indicated in the figure along with the true mean value (μ_{true}) for the natural logarithm of the rate constant (expected value). Gaussian curves using these parameters are shown superimposed on the histograms.

constant are shown in Fig. 4. Gaussian (normal) curves are shown superimposed and the means and standard deviations are indicated along with the actual value of each rate constant. In all cases the estimated mean was very similar to the true value. The greatest discrepancy and the largest relative standard deviation, although still rather small, occurred in the rate constant (k_{12}) which leads to the distal closed state. Because these data sets were calculated at a membrane potential of +30 mV

TABLE 1 Fitted parameters (P), associated estimated parameter errors (EPE) from covariance matrix, and the maximum percent deviation of randomized initial guesses.

	k12 Parameter, EPE EPE % of P	k21 Parameter, EPE EPE % of P	k23 Parameter, EPE EPE % of P	k32 Parameter, EPE EPE % of P
		Two-parameter model		
A	0.024, 9.09	−2.15, 6.77	−0.335, 2.04	−0.801, 11.7
%*	37,500	315	609	1,460
B	0.0028, 0.156	0.058, 0.143	−0.023, 0.030	0.0087, 0.137
%*	5,570	250	130	1,570
		Three-parameter model		
A	1.83, 11.6	−0.732, 10.8	−0.689, 2.29	−0.682, 12.9
%*	630	1,475	300	1,890
B	−0.033, 0.223	0.034, 0.170	−0.023, 0.058	−0.024, 0.120
%*	675	500	250	500
C	−0.000389, 0.00559	−0.0004007, 0.0025	0.000423, 0.00178	0.000846, 0.00343
%*	1,440	625	420	350

*Maximum percent deviation of initial guess away from true value.

where the channels were opening, it is not surprising that this distal closing rate constant would be the least well defined. Note that the natural logarithms of the rate constants, and not the rate constants themselves, were normally distributed. This is because the rate constants are exponential functions of the fitted parameters ($k_{ij} = \exp \{A_{ij} + B_{ij}V + C_{ij}V^2 + \text{error}\}$, see Eq. 6). Because the errors are in the exponent of Eq. 6, they are proportional to the log of the rate constants.

The means and standard deviations of the rate constants expressed as their natural logarithms are shown in Fig. 5 as functions of membrane potential for the two parameter (*top*) and three parameter (*bottom*) expressions for the rate constants. Expressing the rate constants in this manner shows how they change relative to one another as functions of membrane potential. In the log-linear case (Eq. 7; Fig. 5, *top*), the two rate constants leading to the middle closed state showed the most voltage dependence while the other two rate constants were relatively independent of membrane potential. With the more complex parameterization of the rate constants (Eq. 6; Fig. 5, *bottom*), the rate constant leading to the open state (k_{21}) increased with increasing membrane potential but saturated beyond +10 mV. This occurs as the closing rate constants (k_{12} and k_{23}) diminish and the rate constant leading into the open state (k_{32}) became dominant especially > +50 mV. This more complicated voltage dependence would be warranted if the membrane field sensors were induced dipoles in the protein. The standard deviation of each rate constant was usually greatest at one of the voltage limits represented by the simulated data

(−50, +70). The standard deviations of the rate constants were consistently smaller from fits to the 10,000 channel ensemble averages (not shown) than those resulting from fits to the 1,000 channel ensemble averages. The solid lines in Fig. 5 show the actual voltage-dependence of the rate constants used to generate the simulated data sets. The mean rate constants fitted to the simulated data sets were very similar to the actual values, indicating there were no significant inconsistencies between the data generation scheme and the global fitting procedure.

Fig. 6 shows the errors in the rate constants at the 95% confidence limits as a function of transmembrane potential and the number of data sets fitted using the two parameter voltage dependent equation (Eq. 7). Table 2 gives the errors for fits using two or three voltage dependent parameters per rate constant. The three membrane potentials presented in Table 2 (−50, +10, and +70 mV) are representative of the error extremes (best and worst cases). In 92% of the cases shown in Table 2 *A*, the errors were below 20% and were greatest at one of the voltage extremes. When the rate constants were expressed as three parameter functions of membrane potential (Eq. 8, Table 2 *B*), the uncertainty in estimating the rate constants increased. The results indicated that in 79% of the cases the errors were below 30%. In the worst cases (K_{12} and K_{21} at +70 and −50, respectively) the rate constants were still determined within a factor of 2.25. In the simulations using 10,000 channels, the errors in the rate constants fell below 10%.
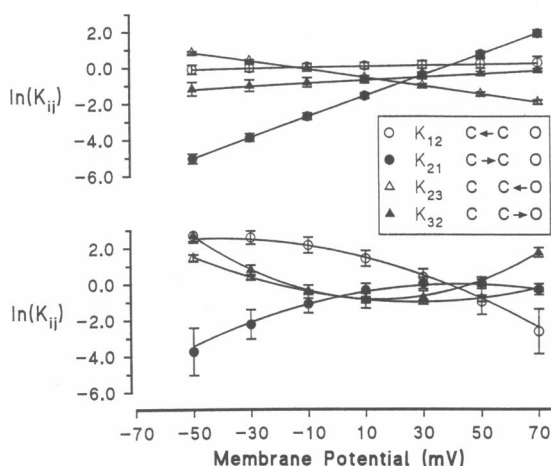

FIGURE 5 The means and standard deviations of the four rate constants are shown superimposed as functions of membrane potential. Results from the two-parameter (*top*) and three-parameter (*bottom*) expressions for the rate constants are shown as their natural logarithms. The solid lines indicate the actual voltage-dependence of the rate constants used to generate the 90 simulations.

DISCUSSION

We have tested a method for extracting rate constants from macroscopic voltage clamp data. We have fitted a published model for the cardiac delayed rectifier (Bennett et al., 1985; Gintant et al., 1985) to macroscopic delayed rectifier currents. This model provided a reasonable approximation of the kinetic features of this channel (Fig. 2). Visual inspection of Fig. 2 suggests that the more complex rate constant parameterization better accommodated the data at +70 mV; however, our objective was not to discriminate among models but to determine if the rate constants could be accurately obtained for a given model. Hence, we did not perform a rigorous statistical comparison of the two models which is beyond the scope of the present paper (see Horn, 1987).

We used the fit to the experimental data set as a basis for performing a Monte Carlo analysis to determine the uncertainty in estimating rate constants using this nonlinear fitting procedure. Fig. 4 indicates that the natural logarithms of the fitted rate constants, and not the rate constants themselves, were normally distributed; hence, the best measure of central tendency was the mean of the
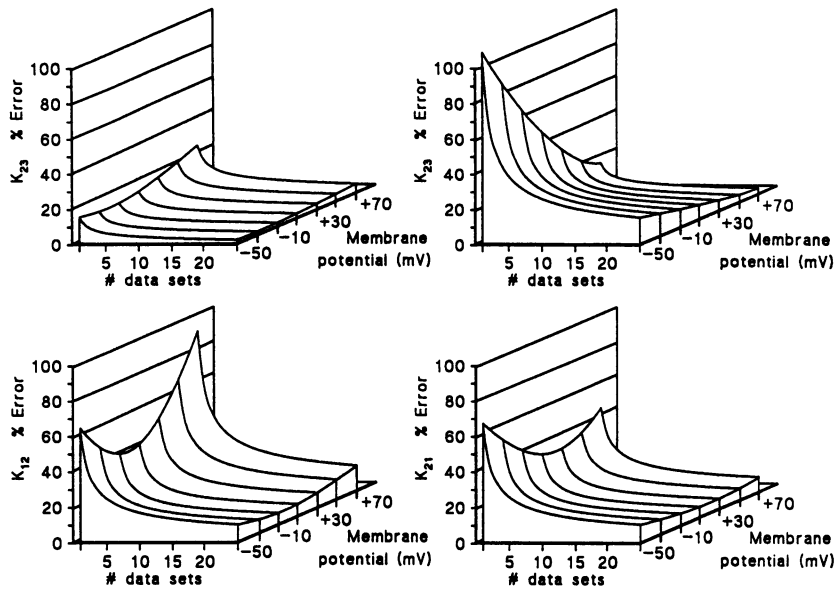
FIGURE 6 The percentage error at the 95% confidence limits as functions of membrane potential and the number of data sets. Errors were calculated for the mean rate constants obtained from global fits to various numbers of data sets, based on the results from the simulations of 1,000 channels. The surfaces plotted were generated by solving the expression shown at the bottom of Table 2.

TABLE 2 **Percentage errors at the 95% confidence limits for each rate constant.**

A: Two-parameter voltage dependence		
Membrane Potential mV	k_{12}	k_{21}
−50	17	18
+10	11	10
+70	22	13
	k_{23} s^{-1}	k_{32} s^{-1}
−50	5	26
+10	5	14
+70	8	5
B: Three-parameter voltage dependence		
Membrane Potential mV	k_{12}	k_{21}
−50	28	125
+10	31	26
+70	116	5
	k_{23} s^{-1}	k_{32} s^{-1}
−50	13	21
+10	5	29
+70	21	17

Errors are shown at three membrane potentials for fits to 10 data sets %
Error = 100* {exp[ln(k_{ij}) + 1.96σ/sqrt(N)] − (k_{ij})}/k_{ij}

natural logarithms of the rate constants resulting from the individual fits. Figs. 5 and 6 both indicate that the uncertainty in parameter estimation usually increased at one or both of the voltage limits covered by the simulated data sets. Notably, the greatest uncertainties were in estimating the forward rate constants (governing opening, k_{32}, k_{21}) at negative membrane potentials where the channels were unlikely to open. The greatest uncertainties in the backward rate constants (k_{12}, k_{23}) were at positive membrane potentials where the channels were least likely to close. Thus as one might predict, the rate constants were least well defined at membrane potentials where they had the least influence on the overall gating behavior. Nevertheless, the mean values obtained provide excellent estimates of the true rate constants used in the simulation.

An interesting observation was that both the forward and reverse rate constants connecting the open state to the first closed state (k_{32} and k_{23}) were voltage dependent in the same direction when the three (Fig. 5, *bottom*) parameter representation of the voltage dependence of the rate constants was used in the fits. However, this figure also shows that their relative magnitudes change dramatically with voltage. At +70 mV the rate constant k_{32} was dominant (*opening direction*). This demonstrates "intuitive" assumptions about the voltage dependence of the rate constants may not be reliable, and that it is the relative magnitude of the rate constants as a function of voltage that dictates the overall behavior of the system. In

the two-parameter model (Eq. 7), the rate constants leading into the middle closed state had the greatest voltage dependence. This suggests that the energy barriers that the channel must overcome to enter this state are influenced by membrane potential. This might occur if there were charged amino acids in a particular region that are driven into new positions by changes in the membrane field. Evidence for such behavior has recently been demonstrated with site directed changes in the protein sequence of the sodium channel by Stuhmer et al. (1989).

The certainty of parameter estimation markedly increased as the number of channels contributing to the simulated ensemble average currents increased from 1,000 to 10,000. The errors decreased by a factor of $\sim 1/\mathrm{sqrt}(10)$ when the number of channels increased by a factor of 10. The standard deviation was 0.327 for ln (k_{12}) in the two-parameter model at +70 mV when 90 fits of 1,000 channels were used; the predicted population standard deviation for 10,000 channels was 0.1034. By fitting nine simulated data sets generated using 10,000 channels each, the calculated standard deviation at +70 mV for ln (k_{12}) was 0.112. In general, the standard deviations obtained from fitting the nine sets of 10,000 channel ensemble averages were greater than the predicted values. This may have resulted in part because we fit only nine of the 10,000 channel simulated data sets, hence the errors overestimated the true population standard deviation with 10,000 channels. The decrease in error with an increase in channel number was a reflection of the improved representation of the mean kinetic behavior of the channel when a larger number of channels contributed to the macroscopic current. Therefore, while this procedure is useful for evaluating the kinetics of channels having low or intermediate membrane density such as the delayed rectifier, the uncertainty of the estimates will decrease when channels with a higher membrane density (e.g., cardiac Na channels) are studied. Thus, in a preparation where the channel density is low, the estimates of the rate constants will be improved by signal averaging. We have utilized this procedure to evaluate the kinetic parameters describing a new model for the cardiac Na channel (Bennett et al., 1989). In that study, the greatest difference between the fitted open state probabilities generated by the parameters of best fit and the whole cell currents was <1%. Furthermore, the fitted kinetic parameters predicted single Na channel kinetic characteristics that agreed with those observed experimentally from single channel recordings.

Fig. 6 suggests that for 1,000 delayed rectifier K channels in the cell membrane, more than five data sets should be fitted to estimate the rate constants to within $\sim 20\%$ of their true values at the voltage extremes. The certainty in the pair of rate constants most distant from

the open state (k_{12} and k_{21}) was greater at membrane potentials near the center of the range covered by the simulated data sets. Thus, kinetic information obtained at one membrane potential to some extent aids in determining kinetic parameters at a nearby membrane potential; hence, parameter estimation at the voltage extremes (here −50 and +70) suffers from having the least amount of overlapping kinetic information from other membrane potentials. Therefore, to accurately assess kinetic behavior at a particular membrane potential, the results suggest that a window of data around the membrane voltage of interest is optimal.

Inclusion of a third term (C_{ij}) describing the voltage dependence of the rate constants (Eq. 6), gave some small visual improvement in the fit (Fig. 2) and reduced the overall residual sum-of-squares, but increased the uncertainty in estimating the individual rate constants. This additional term primarily describes the saturating behavior of the rate constants at the voltage extremes where membrane electrical field induced dipole effects become important. Therefore, addition of data at the voltage extremes (where field-induced dipoles are more likely) or increasing the range of voltages covered by the fitting procedure would be appropriate when these additional kinetic parameters are used.

When the initial guesses were increasingly far from the correct solution, the ability of the global fitting procedure to find the global minimum, or even converge to a solution, decreased. The estimated parameter errors obtained from the inverse of the curvature matrix were quite large relative to the values of the parameters themselves (Table 1); in some cases the error values were two orders of magnitude larger than the fitted parameters. Hence, for the robust analysis, a rather large parameter space was considered. In general, 70% of the cases with initial guesses within 0.25 EPE converged to the global minimum.

In summary, we have fitted a three-state kinetic model to data from voltage clamped potassium current and have tested an approach for extracting rate constants from macroscopic ion channel data. The approach was implemented in a general way to accommodate models with greater complexity as the need arises. We found that there was sufficient information in the macroscopic open channel probability time course to reliably and accurately extract the system rate constants. The Marquardt search algorithm was reasonably robust provided the initial guesses were not extremely bad, however care must be taken to ensure that a global sum-of-squares minimum is achieved. A different search algorithm (e.g., Simplex) may be more robust, but with the cost of additional computation time.

As models with greater complexity are utilized, the uncertainty in determining the kinetic parameters will

increase; however, the use of kinetic observations from well-designed single channel or whole-cell experiments should allow determination of specific rate constants in more complex models, and thereby further extend the utility of this global procedure. Even without additional kinetic information, for more complex models we have found the procedure to be useful for providing an initial set of parameters (rate constants) that serve as a basis for further experimentation and model testing. Our ultimate goal will be to use this method to combine information from single channel, macroscopic ion current and gating current data to obtain a globally optimized set of kinetic model parameters. Thus, an approach that uses both macroscopic and single channel data combined with methods for nonlinear model discrimination, as described by Horn (1987), may provide an objective means for modeling ion channel behavior. These gating models can be used to predict biological behavior that can be further tested experimentally.

REFERENCES

Armstrong, C. M. 1981. Sodium channels and gating currents. *Physiol. Rev.* 61:644–683.

Balser, J. R., and D. M. Roden. 1988. Lanthanum-sensitive current contaminates I_K in guinea pig ventricular myocytes. *Biophys. J.* 53(2):642*a*. (Abstr.)

Bauer, R. J., B. F. Bowman, and J. L. Kenyon. 1987. Theory of the kinetic analysis of patch-clamp data. *Biophys. J.* 52:961–978.

Bennett, P. B., L. C. McKinney, R. S. Kass, and T. Begenisich. 1985. Delayed rectification in the calf cardiac Purkinje fiber: evidence for multiple state kinetics. *Biophys. J.* 48:553–567.

Bennett, P. B., L. C. McKinney, T. Begenisich, and R. S. Kass. 1986. Adrenergic modulation of the delayed rectifier potassium channel in the calf cardiac Purkinje fibers. *Biophys. J.* 49:839–848.

Bennett, P. B., J. R. Balser, L. M. Hondeghem. 1989. A model of the sodium channel: macroscopic and single channel behavior. *Biophys. J.* 55:318*a*. (Abstr.)

Bevington, P. R. 1969. Data Reduction and Error Analysis for the Physical Sciences. McGraw-Hill Book Co., New York. 336 pp.

Caceci, M. S., and W. P. Cacheris. 1984. Fitting curves to data: the simplex algorithm is the answer. *Byte.* May:340–362.

Clapman, D. E., and L. J. DeFelice. 1985. Voltage-activated K channels in embryonic chick heart. *Biophys. J.* 45:40–42.

Colquhoun, D., and A. G. Hawkes. 1983. The principles of the stochastic interpretation of ion-channel mechanisms. *In* Single-Channel Recording. B. Sakmann and E. Neher, editors. Plenum Press, NY. 135–175.

DeFelice, L. J., and J. R. Clay. 1983. Membrane current and membrane potential from single-channel kinetics. *In* Single-Channel Recording. B. Sakmann and E. Neher, editors. Plenum Press, NY. 323–344.

Eyring, H., S. H. Lin, and S. M. Lin. 1980. Basic Chemical Kinetics. Wiley and Sons, New York.

Gear, C. W. 1971. Numerical Initial Value Problems in Ordinary Differential Equations. Prentice-Hall, Englewood Cliffs, NJ.

Gintant, G. A., N. B. Datyner, and I. S. Cohen. 1985. Gating of delayed rectification in acutely isolated canine cardiac Purkinje myocytes: evidence for a single voltage-gated conductance. *Biophys. J.* 48:1059–1064.

Hamill, O. P., A. Marty, E. Neher, S. Sakmann, and F. J. Sigworth. 1981. Improved patch clamp techniques for high-resolution current recording from cells and cell-free membrane patches. *Pfluegers Arch. Eur. J. Physiol.* 391:85–100.

Hammersley, J. M., and D. C. Handscomb. 1964. Monte Carlo methods. Methuen, London.

Hille, B. 1977. Local anesthetics: hydrophilic and hydrophobic pathways for the drug-receptor reaction. *J. Gen. Physiol.* 69:497–515.

Hindmarsh, A. C. 1983. ODEpack, a systematized collection of ODE solvers. *In* Scientific Computing. R. S. Stepleman, editor. North-Holland Co., Amsterdam. 55–64.

Hodgkin, A. L., and A. F. Huxley. 1952. A quantitative description of membrane current and its application to conduction and excitation in nerve. *J. Physiol. (Lond.).* 117:500–544.

Hondeghem, L. M., and B. Katzung. 1977. Time- and voltage-dependent interactions of antiarrhythmic drugs with cardiac sodium channels. *Biochem. et Biophys. Acta.* 472:373–398.

Horn, R. 1987. Statistical methods for model discrimination: application to gating kinetics and permeation of the acetylcholine receptor channel. *Biophys. J.* 51:255–263.

Horn, R., and C. A. Vandenberg. 1984. Statistical properties of single sodium channels. *J. Gen. Physiol.* 84:505–534.

Korn, S. J., and R. Horn. 1988. Statistical discrimination of fractal and Markov models of single-channel gating. *Biophys. J.* 54:871–877.

Kunze, D. L., A. E. Lacerda, D. L. Wilson, and A. M. Brown. 1985. Cardiac Na currents and the inactivating, reopening, and waiting properties of single cardiac Na channels. *J. Gen. Physiol.* 86:691–719.

Liebovitch, L. S., and M. J. Sullivan. 1987. Fractal analysis of a voltage-dependent potassium channel from cultured mouse hippocampal neurons. *Biophys. J.* 52:979–988.

Marquardt, D. W. 1963. An algorithm for least-squares estimation of nonlinear parameters. *J. Soc. Ind. Appl. Math.* 11:431–441.

McManus, O. B., D. S. Weiss, C. E. Spivak, A. L. Blatz, and K. L. Magleby. 1988. Fractal models are inadequate for the kinetics of four different ion channels. *Biophys. J.* 54:859–870.

Mitra, R., and M. Morad. 1985. A uniform enzymatic method for dissociation of myocytes from hearts and stomachs of vertebrates. *Am. J. Physiol.* 249:H1056–1060.

Motulsky, H. J., and L. A. Ransnas. 1987. Fitting curves to data using nonlinear regression: a practical and nonmathematical review. *Fed. Proc.* 1:365–374.

Nelder, J. A., and R. Mead. 1965. A simplex method for function minimization. *Computer J.* 7:308–313.

Petzold, L. R. 1983. Automatic selection of methods for solving stiff and nonstiff systems of ordinary differential equations. *Siam J. Sci. Stat. Comput.* 4:136–148.

Press, W. H., B. P. Flannery, S. A. Teukolsky, and W. T. Vetterling. 1986. Numerical Recipes: The Art of Scientific Computing. Cambridge University Press, Cambridge, UK. 572–577.

Roden, D. M., P. B. Bennett, D. Snyders, J. R. Balser, L. M. Hondeghem. 1988. Quinidine delays I_K activation in guinea pig ventricular myocytes. *Circ. Res.* 62:1055–1058.

Ross, S. M. 1972. Introduction to Probability Models. Academic Press, NY. 272 pp.

Sigworth, F. J. 1980. The variance of sodium current fluctuations at the node of Ranvier. *J. Physiol. (Lond.).* 307:131–142.

Stevens, C. F. 1978. Interactions between intrinsic membrane protein and electric field: an approach to studying nerve excitability. *Biophys. J.* 22:295–306.

Stuhmer, W., F. Conti, H. Suzuki, X. Wang, M. Noda, N. Yahagi, H. Kubo, and S. Numa. 1989. Structural parts involved in activation and inactivation of the sodium channel. *Nature (Lond.).* 339:597–603.